Palaeogeography, Palaeoclimatology, Palaeoecology 285 (2010) 143–151

Contents lists available at ScienceDirect

Palaeogeography, Palaeoclimatology, Palaeoecology

journal homepage: www.elsevier.com/locate/palaeo

A negative carbon isotope excursion defines the boundary from Cambrian Series 2 to Cambrian Series 3 on the Yangtze Platform, South China

Qingjun Guo [a,b,*], Harald Strauss [b], Congqiang Liu [c], Yuanlong Zhao [d], Xinglian Yang [d], Jin Peng [d], Hong Yang [d]

[a] Center for Environmental Remediation, Institute of Geographic Sciences and Natural Resources Research, Chinese Academy of Sciences, Beijing 100101, China
[b] Institut für Geologie und Paläontologie, Westfälische Wilhelms-Universität Münster, Corrensstrasse 24, 48149 Münster, Germany
[c] State Key Laboratory of Environmental Geochemistry, Institute of Geochemistry, Chinese Academy of Sciences, Guiyang 550002, China
[d] Institute of Resource and Environmental Engineering, Guizhou University, Guiyang 550002, China

ARTICLE INFO

Article history:
Received 30 March 2009
Received in revised form 29 September 2009
Accepted 3 November 2009
Available online 10 November 2009

Keywords:
Cambrian Series 2–Cambrian Series 3
Negative carbon isotope excursion
Biology evolution
Jianshan and the Wuliu–Zengjiayan sections
Yangtze Platform

ABSTRACT

A globally recorded negative carbon isotope excursion characterizes the transition from Cambrian Series 2 to Cambrian Series 3. This transition is also well exposed in sedimentary successions on the Yangtze Platform, and the Wuliu–Zengjiayan section, Guizhou Province, South China has been proposed as a potential Global Stratotype Section and Point (GSSP) for this boundary. Here, we report $\delta^{13}C_{carb}$ values for the Jianshan and the Wuliu–Zengjiayan sections. Both sections display a progressive decrease in $\delta^{13}C$ from values around +3‰ upwards in stratigraphy to a pronounced $\delta^{13}C$ minimum with values as low as −6.9‰ at the proposed boundary level, and a return to $\delta^{13}C$ values between 0 and +1‰ in the upper part of the sections. The $\delta^{13}C$ minimum is thought to be caused by a transgressive event, flooding the shelf area with ^{13}C depleted basinal anoxic bottom water. Our $\delta^{13}C$ data are in good agreement with carbon isotope profiles recorded elsewhere. These define the so called ROECE event (*Redlichiid–Oleneliid* Extinction Carbon Isotope Excursion, cf. Zhu et al., 2006, 2007) and may reflect the perturbation of the global carbon cycle during the Cambrian Series 2 to Cambrian Series 3 transition.

1. Introduction

Numerous studies across terminal Neoproterozoic and early Cambrian successions worldwide revealed the great chemostratigraphic potential of high-resolution carbon isotope records (e.g., Brasier et al., 1994; Kaufman and Knoll, 1995; Saltzman et al., 1998; Brasier and Sukhov, 1998; Montañez et al., 2000; Saltzman et al., 2000, 2004). Substantial changes in the carbon isotopic composition of carbonate rocks and organic matter appear to be associated with major faunal boundaries in the Phanerozoic (e.g., Holser and Magaritz, 1987; Magaritz, 1989; Zachos et al., 1989; Saltzman et al., 2000, 2004). The transition from Cambrian Series 2 to Cambrian Series 3 records a rise in global sea level, expressed in large scale transgressive events on the continental landmasses (e.g., Montañez et al., 2000; Hough et al., 2006). High-resolution $\delta^{13}C_{carb}$ records provide a chemostratigraphic framework for the boundary between Cambrian Series 2 and Cambrian Series 3 with previous studies published, e.g., by Donnelly et al. (1988), Brasier (1992), Brasier and Sukhov (1998), Montañez et al. (2000), Zhu et al. (2004), Guo et al. (2005), Wotte et al. (2007), Dilliard et al. (2007), and Shabanov et al. (2008).

A succession of carbonates and siliciclastic sediments across the Cambrian Series 2 to Cambrian Series 3 boundary at the Wuliu–Zengjiayan section, Balang village, Taijiang County, Guizhou Province, South China (Fig. 1) has been proposed as a potential Global Stratotype Section and Point (GSSP) for this boundary (Sundberg et al., 1999; Zhao et al., 2001a, b). Here, we report high-resolution carbonate carbon isotope data for two sections across this interval at Jianshan and Balang, Kaili area, Yangtze Platform, South China. The objective of this study was to investigate the link between $\delta^{13}C$ variations and geological and paleoenvironmental changes of global importance as well as to provide additional data for a global chemostratigraphic subdivision of the boundary from Cambrian Series 2 to Cambrian Series 3.

2. Paleogeographical evolution on the Yangtze Platform

The two sections studied here are located on the Yangtze Platform, South China. During Cambrian times, they were situated in a low latitude position (Fig. 2A). Sediments of the Kaili Formation were deposited in a shelf environment (Fig. 2B) presumably in a water depth between 90 and 300 m (Zhang et al., 1996). The transgressive event proposed for the boundary from Cambrian Series 2 to Cambrian Series 3 resulted in temporal changes in the depositional environment, with parts of the shelf being flooded with less oxygenated basinal bottom waters. This was accompanied by a change in the

* Corresponding author. Center for Environmental Remediation, Institute of Geographic Sciences and Natural Resources Research, Chinese Academy of Sciences, Beijing 100101, China.
E-mail address: guoqingjun@vip.skleg.cn (Q. Guo).

0031-0182/$ – see front matter © 2009 Elsevier B.V. All rights reserved.
doi:10.1016/j.palaeo.2009.11.005

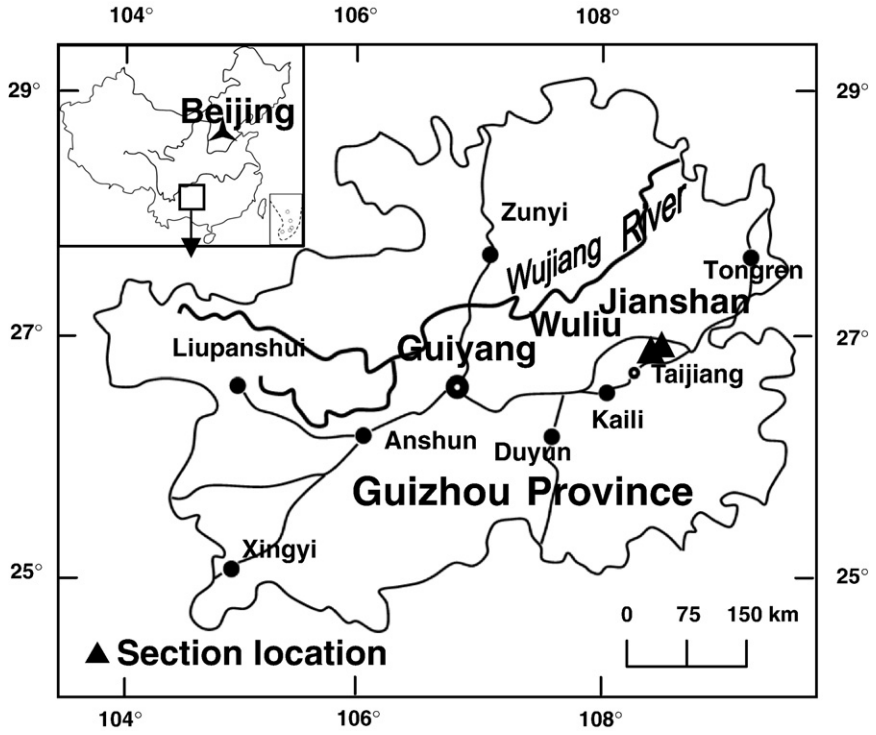

Fig. 1. Map showing the location of the Wuliu–Zengjiayan and Jianshan sections at Balang and Chuandong villages, Guizhou Province, South China.

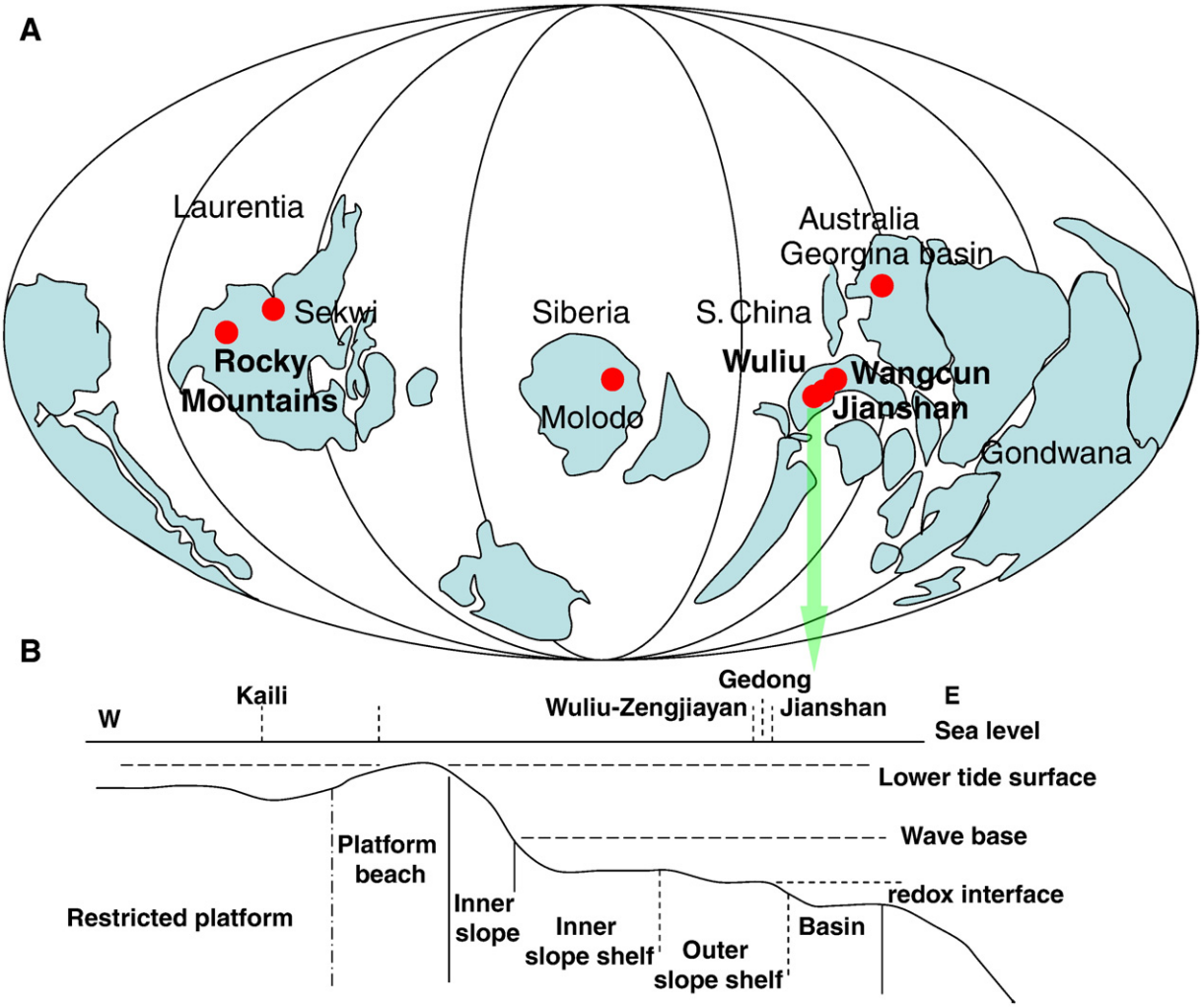

Fig. 2. Paleogeography of the studied successions: (A) Paleogeographic map for the Cambrian (after Scotese and McKerrow, 1990; Saltzman et al., 2000); (B) schematic view of the depositional environment at the studied sections (after Zhang et al., 1996).

pertinent trilobite fauna (e.g., Zhao et al., 2008). The transition from Cambrian Series 2 to Cambrian Series 3 is located at 44.25 m above the base of the Kaili formation in the Jianshan section and at 52.8 m above the base of the Kaili formation at Wuliu–Zengjiayan, based on the First Appearance Datum (FAD) of *Oryctocephalus indicus*.

3. Samples and analytical methods

This study focused on sediments around the boundary from Cambrian Series 2 to Cambrian Series 3 on the Yangtze Platform, South China, specifically from the Jianshan and the Wuliu–Zengjiayan sections (Fig. 1). 37 samples were collected at Jianshan. In addition, and complementary to our previous study (Guo et al., 2005), 26 samples were collected at Balang, extending the published isotope record specifically into the Cambrian Series 3. Lithologies range from pure carbonates to carbonate bearing mudstones.

Prior to geochemical analyses, clean sample interiors were chipped and pulverized (200 mesh). Subsequently, they were analyzed for their total carbon (TC) and total inorganic carbon (TIC) abundances. CO_2 for carbon and oxygen isotope analyses was liberated from whole rock carbonates via off-line phosphorylation (cf. McCrea, 1950) with enriched phosphoric acid (Wachter and Hayes, 1985) at 50 °C for 24 h (limestone) or 48 h (dolomite) and subsequent cryogenic distillation. All carbonate carbon and oxygen isotope analyses were carried out at the Institut für Geologie und Paläontologie in Münster, Germany, using a ThermoFinnigan Delta Plus mass spectrometer. Results are reported in the standard delta notation as $\delta^{13}C$ and $\delta^{18}O$ vs. VPDB. Standard deviation, as determined from replicate analyses, was usually better than 0.15 and 0.20‰ for carbon and oxygen isotopes, respectively.

4. Results

Total inorganic carbon contents for most samples from Jianshan section range between 6 and 12 wt.% with the exception of two mudstone levels at 40–42 m and 57–64 m above section base. $\delta^{13}C$ values for sediments from the Jianshan section range from −6.9 to +3.1‰ ($n=31$)(Fig. 3, Table 1). A clearly discernible stratigraphic variation in $\delta^{13}C$, including a most pronounced minimum in $\delta^{13}C$ at 44 m above the base of section, appears to be independent of TIC values. Mudstones with TIC values below 1.2 wt.% show carbon isotope values between −4.1 and −1.5‰, whereas samples with a TIC value above 6 wt.% are characterized by $\delta^{13}C$ values between −6.9 and +3.1‰. In particular, two samples with extremely ^{13}C-depleted carbon isotope values of −6.9‰ show TIC values of almost 10 wt.%.

The new samples from the Wuliu–Zengjiayan section are characterized by highly variable TIC values ranging between less than 0.1 and almost 12 wt.%. Whole rock carbonate carbon isotope values for these new samples vary between −1.1 and +2.4‰ ($n=26$) (Fig. 3, Table 2), extending the total variation for the entire section to a range

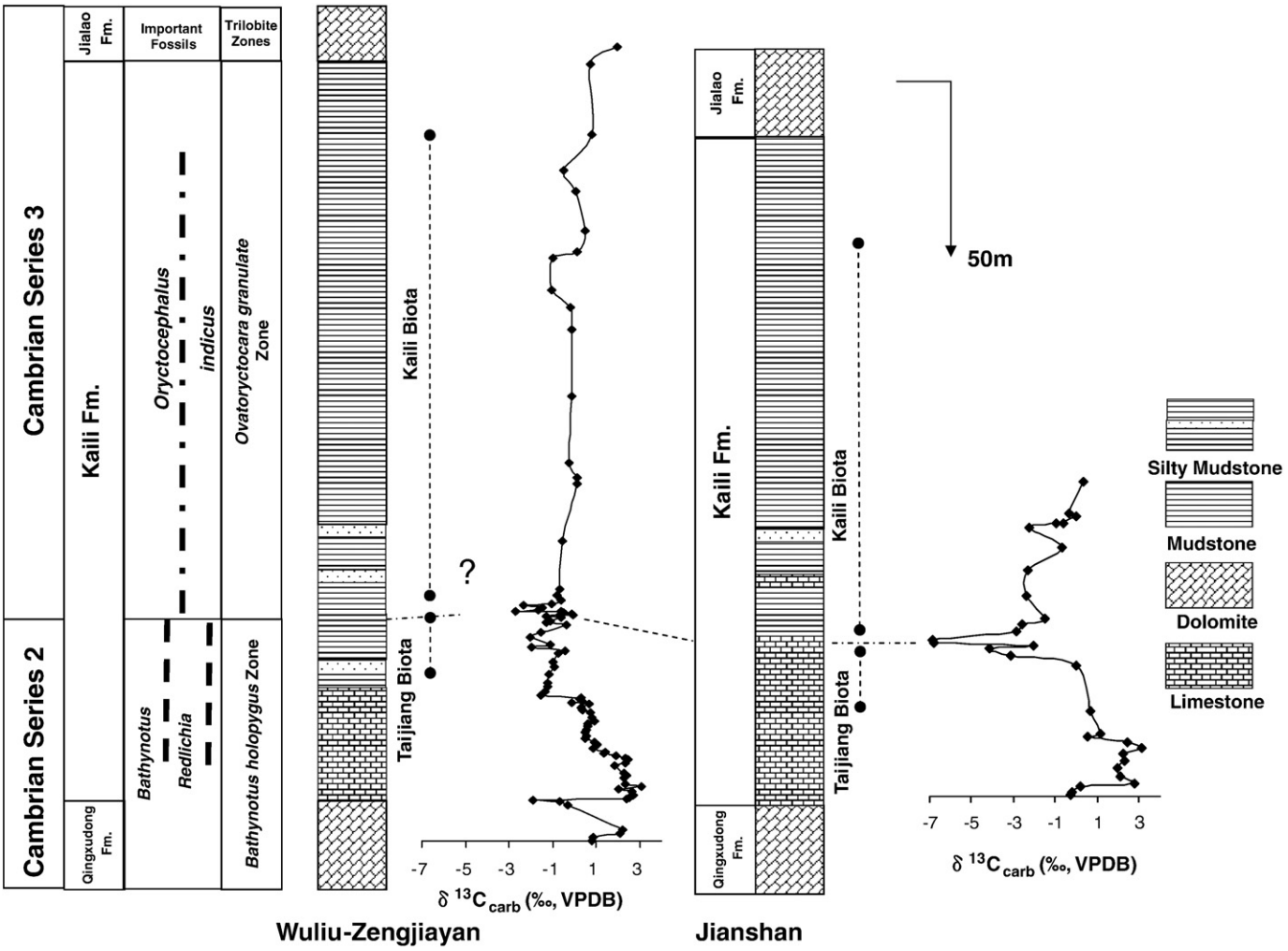

Fig. 3. $\delta^{13}C_{carb}$ profiles for the Wuliu–Zengjiayan and the Jianshan sections, Guizhou Province, Yangtze Platform, South China.

Table 1
Analytical results for sediments from the Jianshan section, Guizhou Province, South China.

Sample	Stratigraphy	Depth (m)	Lithology	$\delta^{13}C_{carb}$ [‰, VPDB]	$\delta^{18}O_{carb}$ [‰, VPDB]	TC (wt.%)	TIC (wt.%)	TOC (wt.%)	TS (wt.%)
CD500	Qingxudong Fm.	0	Dolomite						
CD501	Kaili Fm.	0.3	Limestone	−0.3	−7.7		11.78		
CD502	Kaili Fm.	1.3	Limestone	−0.2	−7.6	11.66	11.08	0.58	0.00
CD503	Kaili Fm.	2.8	Limestone	0.2	−7.6	11.22	10.93	0.29	0.00
CD504	Kaili Fm.	3.8	Limestone	2.8	−7.6	9.47	9.31	0.15	0.32
CD505	Kaili Fm.	5.8	Limestone	2.1	−8.3	8.65	8.05	0.61	0.13
CD506	Kaili Fm.	8.3	Limestone	2.0	−8.5	8.88	8.53	0.35	0.29
CD507	Kaili Fm.	10.3	Limestone	2.3	−8.9	8.58	8.12	0.46	0.08
CD508	Kaili Fm.	12.2	Limestone	2.3	−8.8	8.91	8.38	0.53	0.22
CD509	Kaili Fm.	13.8	Limestone	3.1	−7.3	10.19	9.71	0.48	0.05
CD510	Kaili Fm.	15.5	Limestone	2.5	−7.6	10.48	10.06	0.42	0.00
CD511	Kaili Fm.	17.0	Limestone	0.6	−8.4	7.95	7.55	0.40	0.10
CD512	Kaili Fm.	18.0	Limestone	1.2	−8.1	8.12	7.72	0.40	0.00
CD525	Kaili Fm.	24.4	Limestone	0.7	−7.1	7.67	7.45	0.22	0.01
CD527	Kaili Fm.	37.2	Limestone	0.0	−7.0	8.32	8.01	0.31	0.00
CD528	Kaili Fm.	40.2	Muddy limestone	−3.2	−2.5	1.23	0.57	0.66	0.01
CD530	Kaili Fm.	42.1	Muddy limestone	−4.1	−3.3	0.75	0.50	0.25	0.01
CD531	Kaili Fm.	43.1	Limestone	−2.1	−6.0	1.63	1.14	0.50	0.65
CD513	Kaili Fm.	44.0	Limestone	−6.8	−7.1	9.76	9.74	0.02	0.01
CD513-1	Kaili Fm.	44.7	Limestone	−6.9	−6.4	9.87	9.74	0.14	0.02
CD533	Kaili Fm.	47.1	Calcareous mudstone	−2.8	−4.0	0.62	0.19	0.44	0.01
CD534	Kaili Fm.	49.0	Calcareous mudstone	−2.6	−5.0	0.60	0.42	0.18	0.00
CD535	Kaili Fm.	51.0	Calcareous mudstone	−1.5	−5.6	0.70	0.34	0.36	0.02
CD536	Kaili Fm.	57.5	Calcareous mudstone	−2.4	−4.8	0.79	0.41	0.38	0.01
CD537	Kaili Fm.	64.5	Muddy limestone	−2.3	−5.8	1.47	1.09	0.38	0.01
CD514	Kaili Fm.	71.0	Limestone	−0.7	−8.5	7.94	7.60	0.34	0.00
CD515	Kaili Fm.	76.7	Limestone	−2.3	−7.5	9.24	9.12	0.12	0.00
CD516	Kaili Fm.	78.0	Limestone	−0.6	−9.9	4.44	3.88	0.56	0.40
CD517	Kaili Fm.	78.2	Limestone	−1.0	−7.7	9.08	8.92	0.16	0.00
CD518	Kaili Fm.	80.0	Limestone	0.0	−7.8	9.08	8.75	0.33	0.00
CD519	Kaili Fm.	81.0	Limestone	−0.4	−7.9	8.39	8.30	0.09	0.09
CD521	Kaili Fm.	90.0	Limestone	0.3	−7.7	8.58	6.34	2.24	0.00

from −2.7 to +3.1‰ ($n=90$, including data presented by Guo et al. (2005). Again, a stratigraphic variation in $\delta^{13}C$ is clearly discernible.

5. Discussion

Samples studied from the Jianshan section belong to the Kaili Formation and reflect a stratigraphic profile across the boundary from Cambrian Series 2 to Cambrian Series 3. Chemostratigraphically, the section is characterized by a carbonate carbon isotope trend from values around +2‰ in the lower part to a progressive evolution towards more ^{13}C depleted values. The immediate boundary level between the two Cambrian Series is characterized by a pronounced $\delta^{13}C$ minimum at −6.9‰. Notably, this shift in $\delta^{13}C$ occurs within a thick limestone package and is, hence, independent of lithology. Furthermore, it is independent of respective abundances of total inorganic (ranging from 7.5 to 11.8 wt.%) as well as total organic carbon (below 0.7 wt.%). Moreover, $\delta^{18}O$ values throughout this lower part of the section vary between −8.9 and −6.4‰ ($n=15$) for carbonate samples with TIC values between 6 and 12 wt.%, whereas three mudstones with TIC values below 1.2 wt.% show $\delta^{18}O$ values between −6.0 and −2.5‰. In general, although some diagenetic alteration cannot be excluded, the absence of any clear correlation between parameters considered to represent reliable indicators for a diagenetic overprint (Fig. 4) is taken as evidence that the measured carbonate carbon isotope values have not been altered substantially. Hence, variations in $\delta^{13}C$ are considered to reflect a near-primary signal, including the most pronounced isotopic minimum at the boundary from Cambrian Series 2 to Cambrian Series 3. Following this minimum, $\delta^{13}C$ returns to values around 0‰.

The much thicker Wuliu–Zengjiayan section can be correlated with the succession at Jianshan on the basis of paleontological evidence with a most notable change in the trilobite assemblage defining the boundary (Zhao et al., 2008). The Qingxudong Formation in the lower part of the section displays substantial fluctuations in $\delta^{13}C$, including a minimum value of −1.9‰. The overlying Kaili Formation starts with a limestone package that records a progressive, yet non-linear evolution towards more ^{13}C-depleted carbonate carbon isotope values. This trend continues upwards to the boundary level from Cambrian Series 2 to Cambrian Series 3. The boundary itself, located at 65 m above the base of the section (and 54 m above the base of the Kaili Formation), is characterized by a minimum in the carbonate carbon isotope record, with a $\delta^{13}C$ value of −2.7‰. The boundary is located within a succession of mudstones overlying the limestones of the Kaili Formation and is not associated with any lithological change. Moreover, no strong correlations between carbonate carbon and oxygen as well as between carbonate carbon/oxygen and TIC value are discernible (Tables 1, 2; figures not shown). Again, these observations are collectively taken as evidence that the observed shift in $\delta^{13}C$ is reflecting near-primary variations and are not a result of secondary processes in the diagenetic realm.

Above the Cambrian Series 2 to Cambrian Series 3 boundary, the carbonate carbon signature shifts to $\delta^{13}C$ values around 0‰ and remains more or less invariable for the remaining part of the Kaili Formation.

Further support for our view that the variations in $\delta^{13}C$ reflect a primary signal is provided by the fact that the position of the observed negative shift in $\delta^{13}C$ can be correlated with a similar chemostratigraphic evolution in other sections on the Yangtze Platform (Zhu et al., 2004), in a composite profile across this boundary from the US (Montañez et al., 2000), and in the respective successions in Siberia (Shabanov et al., 2008), and Canada (Dilliard et al., 2007) (Fig. 5). Although differences, both in the magnitude of this shift as well as the absolute minimum $\delta^{13}C$ value exist among the sections studied, the

Table 2
Analytical results for sediments from the Wuliu—Zengjiayan section, Guizhou Province, South China.

Sample	Stratigraphy	Depth (m)	Lithology	$\delta^{13}C_{carb}$ [‰, VPDB]	$\delta^{18}O_{carb}$ [‰, VPDB]	TC (wt.%)	TIC (wt.%)	TOC (wt.%)	TS (wt.%)
1	Qingxudong Fm.	0.0	Dolomite	0.8	−6.8	11.11	10.38	0.73	0.10
2	Qingxudong Fm.	1.0	Dolomite	0.9	−6.2	11.08	10.95	0.12	0.01
3	Qingxudong Fm.	2.0	Dolomite	2.1	−7.6	10.16	9.47	0.69	0.06
4	Qingxudong Fm.	3.0	Dolomite	2.2	−7.7	8.69	7.96	0.74	0.10
5	Qingxudong Fm.	10.0	Dolomite	−0.3	−6.1				0.09
6	Qingxudong Fm.	11.3	Dolomite	−0.7	−6.2	12.53	12.46	0.07	0.03
7	Kaili Fm.	11.6	Limestone	−1.9	−6.5	11.51	11.37	0.13	0.02
8	Kaili Fm.	11.9	Limestone	2.4	−7.2	9.09	8.81	0.28	0.07
9	Kaili Fm.	12.2	Limestone	2.5	−6.9			0.43	0.89
10	Kaili Fm.	13.1	Limestone	2.7	−6.8			0.20	0.10
11	Kaili Fm.	13.9	Limestone	2.7	−6.6			0.42	0.05
12	Kaili Fm.	14.6	Limestone	2.0	−7.2			0.61	0.39
13	Kaili Fm.	15.4	Limestone	3.1	−6.9			0.40	0.21
14	Kaili Fm.	16.1	Limestone	2.4	−7.5			0.41	0.14
15	Kaili Fm.	18.0	Muddy limestone	2.3	−7.5			0.46	0.10
16	Kaili Fm.	18.2	Mudstone			6.50			0.39
17	Kaili Fm.	18.4	Limestone	2.4	−7.5	8.68	8.13	0.56	0.16
18	Kaili Fm.	19.3	Silty limestone	2.3	−7.5			0.94	0.10
19	Kaili Fm.	20.4	Mudstone			6.03			0.50
20	Kaili Fm.	21.3	Limestone	1.9	−6.1	10.46	10.20	0.27	0.01
21	Kaili Fm.	22.2	Muddy limestone	2.4	−7.6			0.48	0.47
22	Kaili Fm.	23.0	Muddy limestone	2.4	−7.8			0.30	0.25
23	Kaili Fm.	23.6	Limestone	2.3	−7.6			0.81	0.18
24	Kaili Fm.	24.3	Muddy limestone	1.9	−7.7			0.52	0.15
25	Kaili Fm.	24.8	Muddy limestone	1.4	−8.3	7.71	7.36	0.35	0.06
26	Kaili Fm.	25.3	Muddy limestone	1.4	−8.2			0.13	
27	Kaili Fm.	26.3	Muddy limestone	0.9	−8.4			0.60	
28	Kaili Fm.	27.3	Muddy limestone	1.1	−8.3			0.09	
29	Kaili Fm.	28.5	Muddy limestone	0.9	−8.0	6.64	6.22	0.42	0.00
30	Kaili Fm.	28.9	Silty limestone	0.5	−8.4	7.24	6.90	0.34	0.00
31	Kaili Fm.	29.8	Silty limestone	0.6	−7.8	7.49	7.49	0.00	0.00
32	Kaili Fm.	30.8	Silty limestone	0.5	−8.4	6.96	6.72	0.24	0.00
33	Kaili Fm.	31.5	Silty limestone	0.6	−8.7	8.05	7.50	0.54	0.00
34	Kaili Fm.	32.4	Silty limestone	0.6	−8.2	6.58	6.09	0.49	0.02
35	Kaili Fm.	33.3	Silty limestone	0.6	−8.4	8.32	8.07	0.26	0.02
36	Kaili Fm.	34.0	Silty limestone	0.9	−8.6	7.60	7.35	0.25	0.00
37	Kaili Fm.	35.0	Silty limestone	0.8	−8.6	7.55	7.30	0.26	0.00
38	Kaili Fm.	36.3	Silty limestone	0.7	−8.1	7.31	7.30	0.01	0.00
39	Kaili Fm.	37.2	Silty limestone	0.4	−7.8	7.07	7.02	0.05	0.00
40	Kaili Fm.	37.9	Silty limestone	0.3	−7.8			0.16	0.02
41	Kaili Fm.	38.8	Silty limestone	0.7	−8.2			0.00	0.01
42	Kaili Fm.	39.3	Silty limestone	−0.1	−8.1	3.17	2.83	0.34	0.01
43	Kaili Fm.	39.7	Silty limestone	0.4	−8.3			0.19	0.02
44	Kaili Fm.	40.3	Muddy limestone	0.2	−8.6	4.41	4.08	0.33	0.01
45	Kaili Fm.	40.6	Silty limestone	0.3	−7.9			0.01	0.02
46	Kaili Fm.	41.3	Mudstone	−1.5	−8.9	1.26	1.08	0.17	0.01
47	Kaili Fm.	42.3	Mudstone	−1.3	−8.7	0.43	0.00	0.43	0.01
48	Kaili Fm.	43.8	Mudstone	−1.2	−8.6	0.33	0.00	0.33	0.01
49	Kaili Fm.	44.8	Mudstone	−1.2	−8.3	1.20	0.83	0.37	0.00
50	Kaili Fm.	47.3	Mudstone	−1.1	−8.7	0.31	0.01	0.30	0.01
51	Kaili Fm.	49.3	Mudstone	−0.9	−8.8	0.36	0.01	0.35	0.01
52	Kaili Fm.	50.8	Mudstone	−1.0	−8.4	0.64	0.31	0.34	0.01
53	Kaili Fm.	51.5	Mudstone						0.02
54	Kaili Fm.	52.5	Mudstone						0.03
55	Kaili Fm.	53.2	Mudstone	−0.7	−9.2			0.16	0.02
56	Kaili Fm.	54.0	Mudstone	−0.4	−9.2	1.24	1.02	0.22	0.01
57	Kaili Fm.	54.9	Mudstone	−2.0	−9.6	0.37	0.14	0.23	0.01
58	Kaili Fm.	55.6	Mudstone	−1.1	−9.0	1.01	0.88	0.13	0.01
59	Kaili Fm.	56.0	Mudstone			0.22			0.02
60	Kaili Fm.	57.0	Mudstone			0.24			0.01
61	Kaili Fm.	57.7	Mudstone	−2.0	−8.3	0.48	0.30	0.18	0.00
62	Kaili Fm.	58.5	Mudstone			0.20			0.00
63	Kaili Fm.	59.2	Mudstone	−1.5	−8.6	0.55	0.37	0.18	0.00
64	Kaili Fm.	59.8	Mudstone			1.39			0.01
65	Kaili Fm.	60.4	Mudstone			0.21			0.01
66	Kaili Fm.	60.9	Mudstone			0.20			0.01
67	Kaili Fm.	61.4	Mudstone	−0.3	−9.3	0.87	0.49	0.38	0.01
68	Kaili Fm.	61.6	Mudstone			0.74			0.01
69	Kaili Fm.	61.8	Mudstone	−1.3	−7.1	0.69	0.40	0.29	0.00
70	Kaili Fm.	62.0	Mudstone			0.57			0.01
71	Kaili Fm.	62.2	Mudstone	−1.1	−7.5	0.50	0.04	0.46	0.01
72	Kaili Fm.	62.4	Mudstone			0.28			0.01
73	Kaili Fm.	62.7	Mudstone			0.17			0.01

(continued on next page)

Table 2 (*continued*)

Sample	Stratigraphy	Depth (m)	Lithology	$\delta^{13}C_{carb}$ [‰, VPDB]	$\delta^{18}O_{carb}$ [‰, VPDB]	TC (wt.%)	TIC (wt.%)	TOC (wt.%)	TS (wt.%)
74	Kaili Fm.	62.9	Mudstone			0.76			0.01
75	Kaili Fm.	63.0	Mudstone			0.20			0.01
76	Kaili Fm.	63.2	Mudstone	−0.6	−9.2	0.45	0.33	0.13	0.01
77	Kaili Fm.	63.4	Mudstone			0.32			0.01
78	Kaili Fm.	63.6	Mudstone	−1.3	−8.4	0.42	0.09	0.33	0.01
79	Kaili Fm.	63.8	Mudstone			0.17			0.01
80	Kaili Fm.	64.0	Mudstone	−0.7	−8.1	0.28	0.00	0.28	0.01
81	Kaili Fm.	64.2	Mudstone	−0.1	−9.9	1.38	1.10	0.28	0.00
82	Kaili Fm.	64.4	Mudstone	−0.1	−9.4	1.75	1.48	0.27	0.00
83	Kaili Fm.	64.6	Mudstone			1.20			0.01
84	Kaili Fm.	64.8	Mudstone	−0.5	−9.4	0.84	0.84	0.00	0.01
85	Kaili Fm.	65.0	Mudstone	−0.6	−9.1	0.53	0.26	0.27	0.00
86	Kaili Fm.	65.2	Mudstone	−2.7	−8.4	0.14	0.14	0.00	0.00
87	Kaili Fm.	65.5	Mudstone	−1.6	−8.4	0.46	0.00	0.46	0.01
88	Kaili Fm.	66.3	Mudstone	−1.5	−8.9	0.59	0.32	0.27	0.01
89	Kaili Fm.	66.7	Mudstone	−2.4	−8.9	0.36	0.27	0.09	0.01
90	Kaili Fm.	67.3	Mudstone	−1.0	−9.1	0.57	0.46	0.11	0.00
91	Kaili Fm.	68.4	Mudstone	−0.6	−8.8	0.72	0.62	0.09	0.01
92	Kaili Fm.	69.6	Mudstone	−0.8	−9.1	0.97	0.92	0.05	0.00
93	Kaili Fm.	71.3	Mudstone	−0.6	−9.1	1.12	1.04	0.08	0.00
94	Kaili Fm.	72.5	Mudstone			0.13			0.00
95	Kaili Fm.	73.6	Mudstone			0.21			0.03
96	Kaili Fm.	74.8	Mudstone			0.43			0.00
97	Kaili Fm.	80.0	Mudstone			0.27	0.26		0.01
98	Kaili Fm.	85.0	Muddy limestone	−0.6	−6.3	0.10	0.00	0.10	0.00
99	Kaili Fm.	101.0	Limestone	0.1	−4.3	5.70	5.46	0.23	0.44
100	Kaili Fm.	102.8	Limestone	0.1	−5.4	5.39	4.56	0.83	0.01
101	Kaili Fm.	107.0	Limestone	−0.2	−7.6			0.00	
102	Kaili Fm.	126.0	Muddy limestone	−0.1	−6.2			0.00	
103	Kaili Fm.	135.0	Mudstone			0.11	0.00	0.11	0.00
104	Kaili Fm.	145.0	Muddy limestone	−0.1	−5.4	0.71	0.55	0.16	0.01
105	Kaili Fm.	151.0	Limestone	−0.2	−3.6	11.22	11.25	−0.04	0.01
106	Kaili Fm.	156.0	Limestone	−1.1	−7.4	7.16	6.93	0.24	0.03
107	Kaili Fm.	165.0	Muddy limestone	−1.0	−5.9	2.76	2.62	0.14	0.00
108	Kaili Fm.	167.0	Limestone	0.1	−6.2	4.70	4.61	0.08	0.04
109	Kaili Fm.	173.0	Limestone	0.5	−6.2	3.06	2.71	0.35	0.23
110	Kaili Fm.	184.0	Limestone	0.1	−7.9	10.16	10.04	0.12	0.02
111	Kaili Fm.	190.0	Limestone	−0.5	−5.2	2.93	2.44	0.49	0.67
112	Kaili Fm.	200.0	Limestone	0.8	−5.7	10.84	10.85	−0.01	0.01
113	Kaili Fm.	220.0	Limestone	0.8	−6.6	11.66	11.25	0.41	0.03
114	Jialao Fm.	225.0	Dolomite	2.0	−7.6	10.07	9.15	0.93	0.07

boundary from Cambrian Series 2 to Cambrian Series 3, in principle defined on the basis of a trilobite mass extinction event (*Ovatoryctocara granulate–Bathynotus holopygus* zone), is also associated with a punctuated negative shift in $\delta^{13}C$, the so called *Redlichiid–Olenellid* Extinction Carbon isotope Excursion (ROECE; Zhu et al., 2006, 2007). Based on the data presented here, this distinct negative excursion in the uppermost part of Cambrian Series 2 and lowermost part of Cambrian Series 3 is occurring in successions from Gondwana and Laurentia.

Major changes in paleogeography coupled to the rise in sea level have been discussed in connection with the trilobite mass extinction and the negative carbon isotope excursion (e.g., Montañez et al., 2000) at the ROECE event. As mentioned above, this rise in sea level caused the deposition of transgressive successions visible in Laurentian and Siberian sections (e.g., Brasier and Sukhov, 1998; Landing and Bartowski, 1996; Montañez et al., 2000). On the Yangtze Platform of South China, this is expressed by the carbonate–shale successions that were studied here. Apart from carbon, Hough et al. (2006) discussed a short-term high magnitude shift in the sulfur isotopic composition of seawater sulfate towards positive $\delta^{34}S$ values. They relate this shift to the spread of anoxic bottom water conditions during the Cambrian Series 2 to Cambrian Series 3 transition, and speculate about a connection to the emplacement of a large igneous province at that time. The development of inhospitable bottom water conditions due to the introduction of anoxic waters would undoubtedly result in faunal extinction. Observed differences in the magnitude of the $\delta^{13}C$ shift between different sections on the Yangtze Platform and worldwide could very well reflect an additional influence on the carbonate carbon isotopic composition of more regional/local importance, superimposed on the global signal.

In linking the carbonate carbon isotope signature with assumed pertinent paleogeographical changes, we propose an environmental model (Fig. 6) that provides an explanation for the observed temporal changes in biogeochemistry. High $\delta^{13}C_{carb}$ values around +3‰, measured for carbonates in the lower part of the Kaili Formation in both profiles, attest to a high demand for dissolved inorganic carbon during autotrophic carbon fixation in the oxygenated surface waters and/or the enhanced burial of organic carbon. On the Yangtze Platform, the oxygenated waters provide the habitat for the Taijiang Fauna (Zhao et al., 1998). Whether or not anoxic bottom water conditions prevailed in the outer shelf and deeper water environments cannot be ascertained based on the profiles studied. Throughout the lower part of the Kaili Formation, approaching the boundary from Cambrian Series 2 to Cambrian Series 3, $\delta^{13}C$ values decrease to minimum values at the level which — based on paleontological evidence — has been suggested to mark the immediate boundary level. Assuming that the observed decrease in $\delta^{13}C$ is not caused by progressive diagenetic alteration, for which there is no evidence, this evolution records the progressive change in the carbon isotopic composition of dissolved inorganic carbon in the water column that is utilized for carbonate precipitation.

In terms of global carbon cycling, decreasing carbon isotope values could either reflect a decrease in carbon fixation and/or a decrease in organic carbon burial (e.g., Hayes et al., 1999). Alternatively and/or in

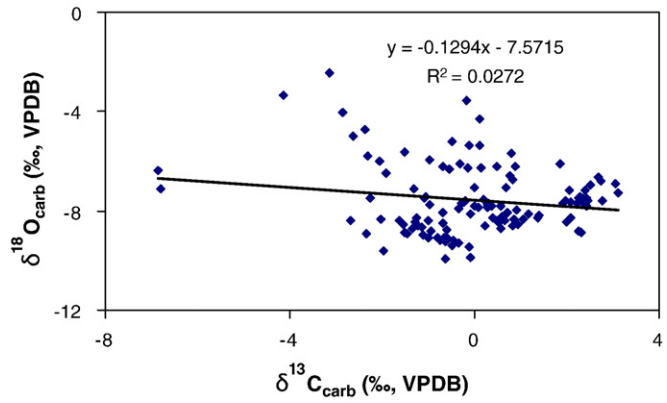

Fig. 4. Cross-plot of $\delta^{13}C_{carb}$ and $\delta^{18}O_{carb}$ for all samples.

addition, the upwelling of water with dissolved inorganic carbon carrying a ^{13}C depleted signature due to recycling of organic matter or enhanced weathering of organic carbon bearing rocks on the continents and subsequent delivery of ^{13}C depleted dissolved inorganic carbon into the ocean, could be responsible for the observed change in $\delta^{13}C$. In accordance with a proposed rise in global sea level and the transgressive flooding of continental areas, the recorded decrease in $\delta^{13}C$ is interpreted to reflect the progressive flushing of anoxic bottom waters with a negative carbon isotope signature for dissolved inorganic carbon from deeper water areas previously located on the outer shelf to the inner shelf area of the Yangtze Platform. This signature was then incorporated into subsequently precipitating carbonate. When comparing the two studied sections, observed differences in the absolute $\delta^{13}C$ values for the carbon isotope minima are viewed to record regional/local conditions superimposed on the global carbon isotope evolution. The generally more ^{13}C depleted signature for samples from the Jianshan section could reflect a closer proximity to the source of ^{13}C depleted water during upwelling.

Following the $\delta^{13}C$ minimum, carbon isotope values increase again to slightly positive values, indicating the recovery of the system. The sediments of the upper Kaili Formation (Cambrian Series 3) are characterized by $\delta^{13}C$ values around 0‰, well in accordance with carbon isotope data recorded by Zhu et al. (2004) for another section on the Yangtze Platform.

6. Conclusions

New carbonate carbon isotope profiles across the boundary from the Cambrian Series 2 to the Cambrian Series 3, measured for two sedimentary successions on the Yangtze Platform, display clear temporal variations in $\delta^{13}C$. Most notably is a carbon isotope

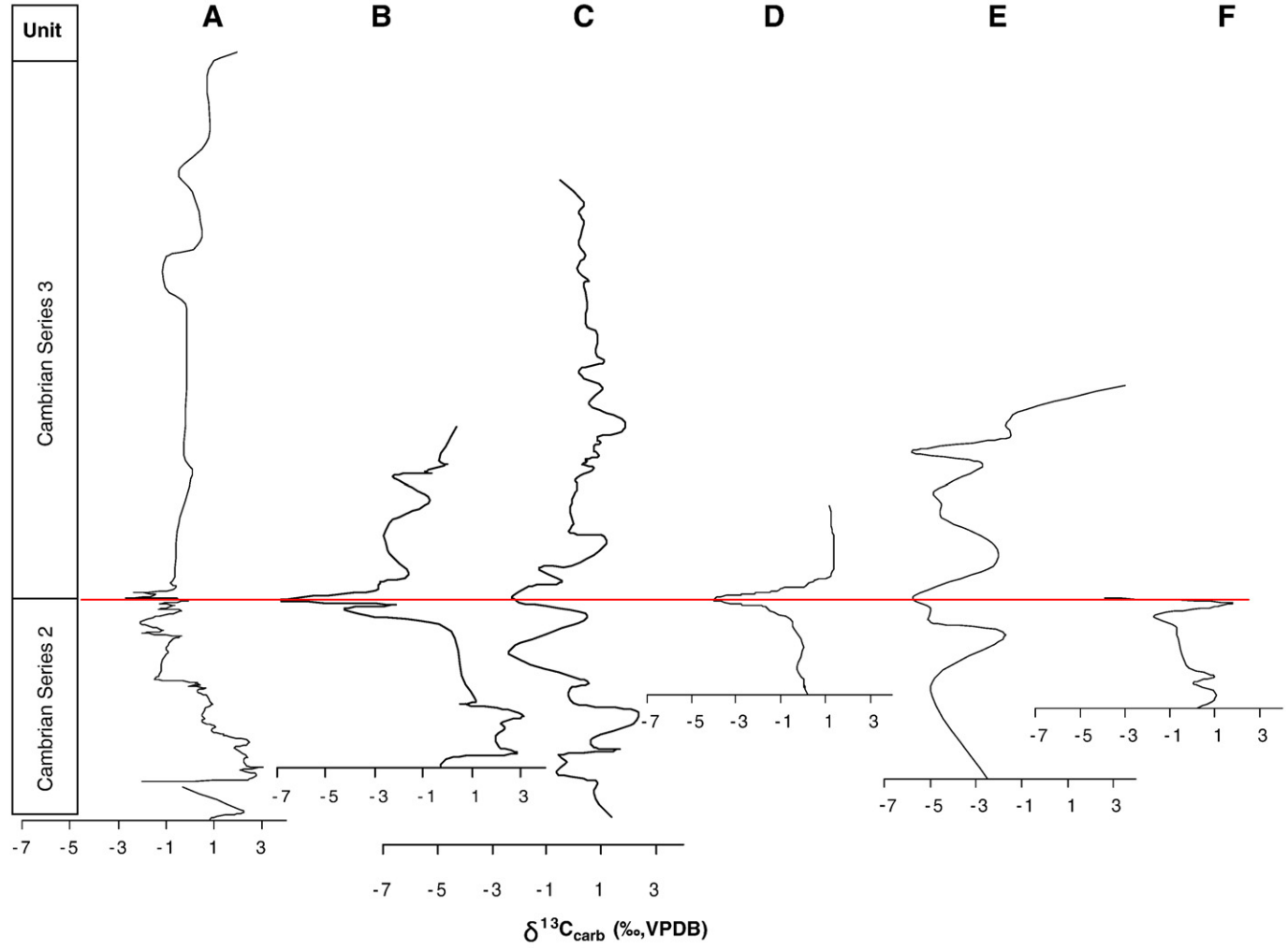

Fig. 5. Comparison of temporal variations in $\delta^{13}C_{carb}$ across the boundary from Cambrian Series 2 to Cambrian Series 3 (A) Wuliu–Zengjiayan section, China (this study), (B) Jianshan section, China (this study), (C) Wangcun section, China (Zhu et al., 2004), (D) Rocky Mountain section, USA (Montañez et al., 2000), (E) Molodo section, Russia (Shabanov et al., 2008) and (F) Sekwi Formation, Canada (Dilliard et al., 2007).

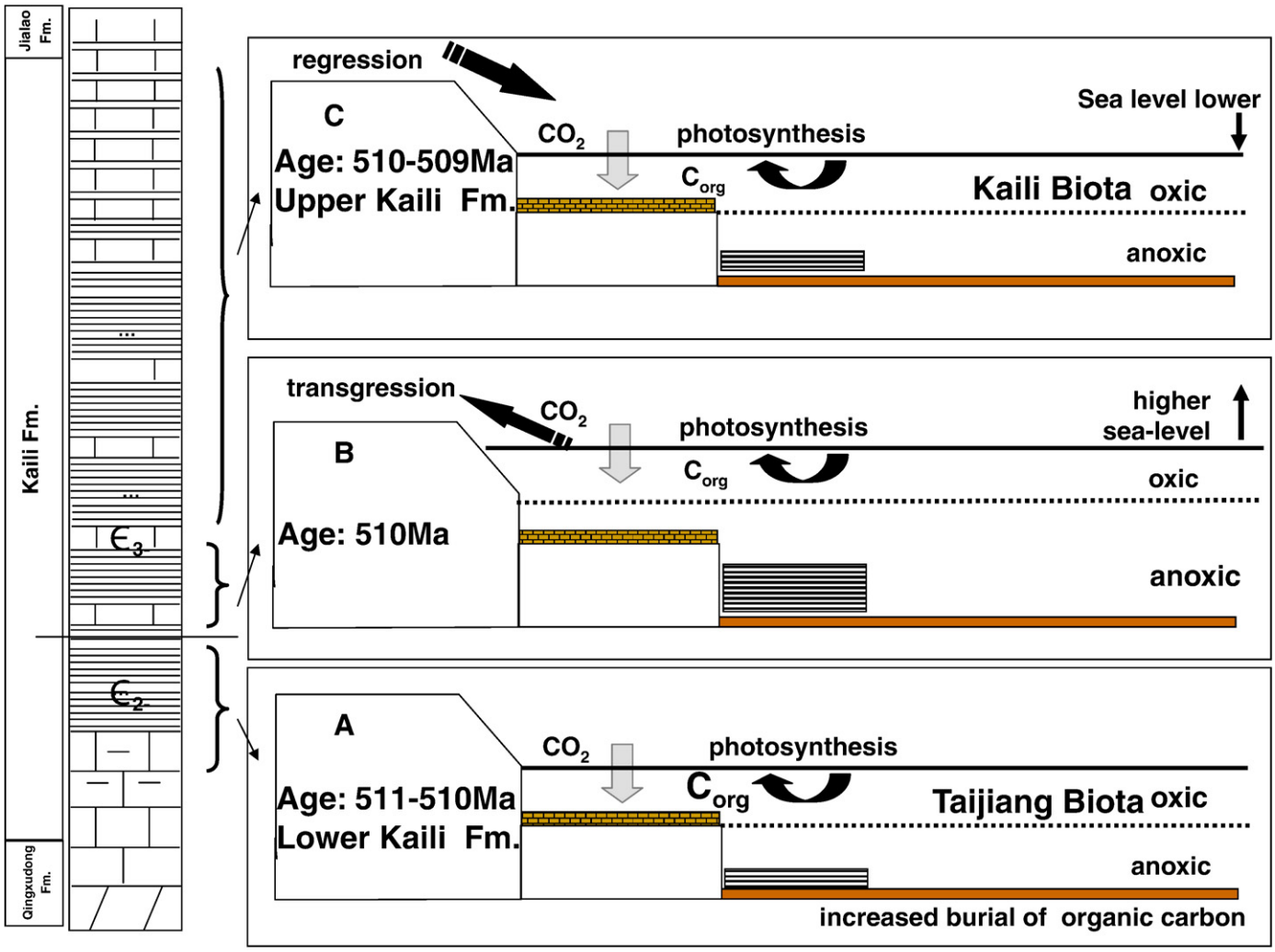

Fig. 6. Environmental evolution across the transition from Cambrian Series 2 to Cambrian Series 3.

minimum at a level in stratigraphy that coincides with the paleontologically defined boundary between these two Cambrian series. The carbon isotopic evolution recorded for the sections at Jianshan and at Wuliu–Zengjiayan is in good agreement with existing $\delta^{13}C$ records obtained from other sections on the Yangtze Platform and on other continents that define the ROECE event. This strengthens the case that the carbon isotope trend truly observed in the two sections studied here reflects perturbations of the global carbon cycle. The global signature, however, has been enhanced by a more regional signal, likely as a consequence of differences in the paleogeographical setting.

Acknowledgements

We wish to sincerely thank Prof. Dr. Zhu Maoyan, Prof. Peng Shanchi, Prof. Dr. Yuan Jinliang, Dr. Thomas Wotte and Mr. Artur Fugmann for discussion and for assistance and expertise in the field and the laboratory. Financial support by the Alexander von Humboldt Foundation, NSFC (Nos. 40672008, 40972023, 40930211), DFG (No. Str 281/16-1/16-2), One Hundred Person Project of the Chinese Academy of Sciences and 973 Program (2006CB806401), the key project of international cooperation of Guizhou Science and Technology (Gui. Co.G.[2008]700110]), the Foundation of Science and Technology of Guizhou Province (Grant No. Gui J. 2007-2151, 2007-4004), and the Doctor Foundation of Guizhou University is gratefully acknowledged. Reviews of this manuscript by Prof. David J. Bottjer, Prof. Yanan Shen and an anonymous reviewer are gratefully acknowledged.

References

Brasier, M.D., 1992. Towards a Carbon Isotope Stratigraphy of the Cambrian System: Potential of the Great Basin Succession. In: Hailwood, E.A., Kidd, R.B. (Eds.), High Resolution Stratigraphy: Geological Society Special Publication, 70, pp. 341–350.

Brasier, M.D., Sukhov, S.S., 1998. The falling amplitude of carbon isotopic oscillations through the Lower to Middle Cambrian: northern Siberia data. Canadian Journal of Earth Sciences 35, 353–373.

Brasier, M.D., Rozanov, A.Yu., Zhuravlev, A.Yu., Corfield, R.M., Derry, L.A., 1994. A carbon isotope reference scale for the Lower Cambrian succession in Siberia: report of IGCP Project 303. Geological Magazine 131, 767–783.

Dilliard, K.A., Pope, M.C., Coniglio, M., Hasiotis, S.T., Lieberman, B.S., 2007. Stable isotope geochemistry of the lower Cambrian Sekwi Formation, Northwest Territories, Canada: implications for ocean chemistry and secular curve generation. Palaeogeography Palaeoclimatology Palaeoecology 256, 174–194.

Donnelly, T., Shergold, J.H., Southgate, P.N., 1988. Anomalous geochemical signals from phosphatic Middle Cambrian rocks in the southern Georgina Basin, Australia. Sedimentology 35, 549–570.

Guo, Q., Strauss, H., Liu, C., Zhao, Y., Pi, D., Fu, P., Zhu, L., Yuan, J., 2005. Carbon and oxygen isotopic composition of Lower to Middle Cambrian sediments at Taijiang, Guizhou Province, China. Geological Magazine 142, 723–733.

Hayes, J.M., Strauss, H., Kaufman, A.J., 1999. The abundance of ^{13}C in marine organic matter and isotopic fractionation in the global biogeochemical cycle of carbon during the past 800 Ma. Chemical Geology 161, 103–125.

Holser, W.T., Magaritz, M., 1987. Events near the Permian–Triassic boundary. Modern Geology 11, 155–180.

Hough, M.L., Shields, G.A., Evins, L.Z., Strauss, H., Henderson, R.A., Mackenzie, S., 2006. A major sulphur isotope event at 510 Ma: a possible anoxia-extinction-volcanism connection during the Early–Middle Cambrian transition? Terra Nova 18, 257–263.
Kaufman, A.J., Knoll, A.H., 1995. Neoproterozoic variations in the C-isotopic composition of seawater: stratigraphic and biogeochemical implications. Precambrian Research 73, 27–49.
Landing, E., Bartowski, K.E., 1996. Oldest shelly fossils from the Taconic allochthon and late Early Cambrian sea-levels in eastern Laurentia. Journal of Paleontology 70, 741–761.
Magaritz, M., 1989. ^{13}C minima follow extinction events: a clue to faunal extinction. Geology 17, 337–340.
McCrea, J.M., 1950. On the isotopic chemistry of carbonates and a paleotemperature scale. Journal of Chemical Physics 18, 849–857.
Montañez, I.P., Osleger, D.A., Banner, J.L., Mack, L.E., Masgrove, M.L., 2000. Evolution of the Sr and C isotope composition of Cambrian oceans. GSA Today 10, 1–7.
Saltzman, M.R., Runnegar, B., Lohmann, K.C., 1998. Carbon isotope stratigraphy of Upper Cambrian (Steptoean Stage) sequences of the eastern Great Basin: record of a global oceanographic event. Geological Society of America Bulletin 110, 285–297.
Saltzman, M.R., Ripperdan, R.L., Brasier, M.D., Lohmann, K.C., Robison, R.C., Chang, W.T., Peng, S., Ergaliev, E.K., Runnegar, B.R., 2000. A global carbon isotope excursion (SPICE) during the Late Cambrian: relation to trilobite extinction, organic-matter burial, and sea level. Palaeogeography, Palaeoclimatology, Palaeoecology 160, 211–223.
Saltzman, M.R., Runkel, A.C., Cowan, C.A., Runnegar, B., Stewart, M.C., Palmer, A.R., 2004. The upper Cambrian SPICE ($\delta^{13}C$) event and the Sauk II–Sauk III regression: new evidence from Laurentian basins in Utah, Iowa and Newfoundland. Journal of Sedimentary Research 74, 366–377.
Scotese, C.R., McKerrow, W.S., 1990. Revised world maps and introduction. Geological Society, London, Memoir 12, 1–21.
Shabanov, Yu.Ya., Korovnikov, I.V., Pereladov, V.S., Pak, K.L., Feflov, A.F., 2008. The section of the Kuonamka Formation of the Molodo River — a candidate for a global stratigraphy of the lower boundary of the Middle Cambrian (East Siberian Platform). Cambrian sections of the Siberian Platform — stratotype candidates for an international stratigraphic scaling (Stratigraphy and Palaeontology). Material of the 13th International Field Conference of the Cambrian Subdivision Working Group. Yakutia, pp. 60–70.
Sundberg, F.A., Yuan, J., McCollum, L.B., Zhao, Y., 1999. Correlation of the Lower–Middle Cambrian boundary of South China and Western United State of America. Acta Palaeontologica Sinica 38, 102–107.
Wachter, E.A., Hayes, J.M., 1985. Exchange of oxygen isotopes and carbon isotopes in carbon dioxide-phosphoric acid systems. Chemical Geology 52, 365–374.
Wotte, T., Álvaro, J.J., Shields, G.A., Brown, B., Brasier, M.D., Veizer, J., 2007. C-, O- and Sr-isotope stratigraphy across the Lower–Middle Cambrian transition of the Cantabrian Zone (Spain) and the Montagne Noire (France), West Gondwana. Palaeogeography, Palaeoclimatology, Palaeoecology 256, 47–70.
Zachos, J.C., Arthur, M.A., Dean, W.E., 1989. Geochemical evidence for suppression of pelagic marine productivity at the Cretaceous/Tertiary boundary. Nature 337, 61–64.
Zhao, Y., Yuan, J., Zhu, M., Huang, Y., Guo, Q., Yang, R., Zhou, Z., 1998. Early Cambrian Taijiang Fauna in Taijiang County, Guizhou, China. Journal of Guizhou University of Technology 27 (5), 23–26.
Zhao, Y., Yuan, J., Zhu, L., Guo, Q., Yang, R., Yang, X., 2001a. A progress report on research and prospects of the Lower–Middle Cambrian boundary in China. Journal of Stratigraphy 25, 376–383.
Zhao, Y., Yuan, J., McCullum, L.B., Sundberg, F.A., Yang, R., Guo, Q., Zhu, L., Yang, X., 2001b. A potential GSSP for the Lower and Middle Cambrian boundary near Balang village, Taijiang county, Guizhou Province, China. Acta Palaeontological Sinica 40, 130–142.
Zhao, Y., Yuan, J., Peng, S., Loren, E.B., Peng, J., Guo, Q., Lin, J., Tai, T., Yang, R., Wang, Y., 2008. A new section of Kaili Formation (Cambrian) and a biostratigraphic study of the boundary interval across the undefined Cambrian Series 2 and Series 3 at Jianshan, Chuandong village, Jianhe County, China with a discussion of global correlation based on the first appearance datum of *Oryctocephalus indicus* (Reed, 1910). Progress in Natural Science 18, 1549–1556.
Zhang, Z., Shen, J., Gong, X., Zhao, Y., 1996. A preliminary discussion on preservation condition of Kaili Fauna, Middle Cambrian, Taijiang, Guizhou. Acta Palaeontologica Sinica 35 (5), 607–622.
Zhu, M., Zhang, J., Li, G., Yang, A., 2004. Evolution of C isotopes in the Cambrian of China: implications for Cambrian subdivision and trilobite mass extinctions. Geobios 37, 287–301.
Zhu, M., Babcock, L.E., Peng, S., 2006. Advances in Cambrian Stratigraphy and paleontology: integrating correlation techniques, palaeobiology, taphonomy and paleoenvironmental reconstruction. Palaeoworld 15, 217–222.
Zhu, M., Zhang, J., Yang, A., 2007. Integrated Ediacaran (Sinian) chronostratigraphy of South China. Palaeogeography, Palaeoclimatology, Palaeoecology 254, 7–61.